Mms1 and Mms22 stabilize the replisome during replication stress

Jessica A. Vaisica[a,b], Anastasija Baryshnikova[b,c], Michael Costanzo[b,c], Charles Boone[b,c], and Grant W. Brown[a,b]

[a]Department of Biochemistry, University of Toronto, Toronto, ON M5S 1A8, Canada; [b]Donnelly Centre for Cellular and Biomolecular Research, University of Toronto, Toronto, ON M5S 3E1, Canada; [c]Banting and Best Department of Medical Research and Department of Molecular Genetics, University of Toronto, Toronto, ON M5G 1L6, Canada

ABSTRACT **Mms1 and Mms22 form a Cul4^{Ddb1}-like E3 ubiquitin ligase with the cullin Rtt101. In this complex, Rtt101 is bound to the substrate-specific adaptor Mms22 through a linker protein, Mms1. Although the Rtt101$^{Mms1/Mms22}$ ubiquitin ligase is important in promoting replication through damaged templates, how it does so has yet to be determined. Here we show that *mms1*Δ and *mms22*Δ cells fail to properly regulate DNA replication fork progression when replication stress is present and are defective in recovery from replication fork stress. Consistent with a role in promoting DNA replication, we find that Mms1 is enriched at sites where replication forks have stalled and that this localization requires the known binding partners of Mms1—Rtt101 and Mms22. Mms1 and Mms22 stabilize the replisome during replication stress, as binding of the fork-pausing complex components Mrc1 and Csm3, and DNA polymerase ε, at stalled replication forks is decreased in *mms1*Δ and *mms22*Δ. Taken together, these data indicate that Mms1 and Mms22 are important for maintaining the integrity of the replisome when DNA replication forks are slowed by hydroxyurea and thereby promote efficient recovery from replication stress.**

Monitoring Editor
Orna Cohen-Fix
National Institutes of Health

Received: Oct 26, 2010
Revised: Apr 19, 2011
Accepted: May 6, 2011

INTRODUCTION

Faithful transmission of the genome from one generation to the next requires the accurate and timely replication of the DNA. Accurate DNA replication requires a complex of proteins that localize to the replication fork, collectively referred to as the replisome (Aparicio *et al.*, 1997; Tercero *et al.*, 2000; Calzada *et al.*, 2005). Key components of the replisome include Cdc45-MCM-GINS (CMG) which likely compose the replicative DNA helicase (Aparicio *et al.*, 1997; Tercero *et al.*, 2000; Zou and Stillman, 2000; Takayama *et al.*, 2003; Gambus *et al.*, 2006) Polα-primase, which primes the leading strand and Okazaki fragments (Plevani *et al.*, 1984; Singh and Dumas, 1984), the leading and lagging-strand polymerases (Polε and PolΔ; Pursell *et al.*, 2007; Nick McElhinny *et al.*, 2008), Ctf4 and Mcm10, which interact with Polα-primase (Ricke and Bielinsky, 2004; Gambus *et al.*, 2009; Tanaka *et al.*, 2009), and the replication fork–pausing complex (FPC), which comprises Mrc1, Csm3, and Tof1 (Katou *et al.*, 2003; Noguchi *et al.*, 2004; Calzada *et al.*, 2005; Nedelcheva *et al.*, 2005; Szyjka *et al.*, 2005; Bando *et al.*, 2009).

The timely progression of DNA replication forks can be challenged by a number of conditions, including nucleotide base lesions, abasic sites, interstrand and intrastrand cross-links, DNA secondary structures, sites of strong protein–DNA interactions, transcription complexes, depletion or inhibition of DNA polymerases, and depletion of dNTPs. These challenges are collectively referred to as replication stress. Replication stress is readily induced experimentally by the ribonucleotide reductase inhibitor hydroxyurea (Krakoff *et al.*, 1968; Slater, 1973; Alvino *et al.*, 2007), which results in a depletion of deoxyribonucleotide triphosphates (dNTPs), thereby causing a large decrease in replication fork rate. Hydroxyurea (HU) also activates a cell cycle checkpoint (Weinert *et al.*, 1994), which delays cell cycle progression until S phase is complete, stabilizes replication fork proteins at the stalled or slowed forks, and promotes the ability of replication forks to complete DNA synthesis (Desany *et al.*, 1998; Alcasabas *et al.*, 2001; Lopes *et al.*, 2001; Sogo *et al.*, 2002; Cobb *et al.*, 2003; Katou *et al.*, 2003; Osborn and

This article was published online ahead of print in MBoC in Press (http://www.molbiolcell.org/cgi/doi/10.1091/mbc.E10-10-0848) on May 18, 2011.

Address correspondence to: Grant W. Brown (grant.brown@utoronto.ca).

Abbreviations used: αF, alpha factor; ARS, autonomously replicating sequence; replication origin; BrdU, bromodeoxyuridine; BrdU-IP chip, BrdU immunoprecipitation on tiling microarray; ChIP, chromatin immunoprecipitation; ChIP-chip, chip on tiling microarray; dNTP, deoxyribonucleoside triphosphate; FPC, fork-pausing complex; HU, hydroxyurea; IP, immunoprecipitation; MMS, methyl methanesulfonate; nt, nucleotide; qPCR, quantitative PCR.

Elledge, 2003; Tercero *et al.*, 2003; Lucca *et al.*, 2004; Bjergbaek *et al.*, 2005; Feng *et al.*, 2006; Naylor *et al.*, 2009; Tittel-Elmer *et al.*, 2009). Although the mechanisms by which the checkpoint stabilizes replisomes under conditions of replication stress and promotes DNA replication are not entirely known, there are a number of connections between replisome components and the checkpoint. Replisome destabilization has been noted in deletion mutants of several genes with roles in maintaining genome integrity. Deletion of *MEC1*, *RAD53*, or *SGS1* decreases the association of DNA polymerases with stalled forks (Cobb *et al.*, 2005), as does deletion of *MRC1* and genes encoding components of the MRX complex (Lou *et al.*, 2008; Tittel-Elmer *et al.*, 2009). In addition, deletion of *MRC1*, *CSM3*, *TOF1*, *DIA2*, and *CTF4* each causes replisome migration to become uncoupled from the nascent DNA chain (Katou *et al.*, 2003; Bando *et al.*, 2009; Mimura *et al.*, 2009; Tanaka *et al.*, 2009). These data indicate that a complex network of proteins functions to maintain the integrity of the replisome at the DNA replication fork when cells encounter replication stress.

In budding yeast the genes *MMS1* and *MMS22* are important for resistance to replication stress, either from dNTP depletion by HU or by DNA damage induced by methyl methanesulfonate (MMS) or camptothecin (Bennett *et al.*, 2001; Chang *et al.*, 2002; Hryciw *et al.*, 2002; Araki *et al.*, 2003; Baldwin *et al.*, 2005; Dovey and Russell, 2007; Dovey *et al.*, 2009; Yokoyama *et al.*, 2007; Roberts *et al.*, 2008). Genetic interaction data suggest that Mms1 and Mms22 function with the cullin Rtt101 (Pan *et al.*, 2006; Collins *et al.*, 2007; Costanzo *et al.*, 2010; Koh *et al.*, 2010). Consistent with these data, *rtt101*Δ shares many phenotypes with *mms1* and *mms22* deletion mutants. Similar to *mms1*Δ and *mms22*Δ strains, *rtt101*Δ cells are sensitive to agents that perturb replication and induce DNA damage (Chang *et al.*, 2002; Luke *et al.*, 2006; Roberts *et al.*, 2008). Deletion mutants of *rtt101* also have increased rates of spontaneous DNA damage during a normal cell cycle (Luke *et al.*, 2006), accumulate at the G2/M transition (Michel *et al.*, 2003), and display an abnormal nuclear morphology (Michel *et al.*, 2003; Luke *et al.*, 2006), much like *mms1*Δ and *mms22*Δ (Dovey and Russell, 2007; Dovey *et al.*, 2009; Yokoyama *et al.*, 2007; Duro *et al.*, 2008; Roberts *et al.*, 2008).

Protein–protein interactions also suggest that Mms1 and Mms22 function in concert with Rtt101 (Ho *et al.*, 2002; Pan *et al.*, 2006; Suter *et al.*, 2007; Zaidi *et al.*, 2008; Ben-Aroya *et al.*, 2010; Mimura *et al.*, 2010), and sequence conservation further suggests that $Rtt101^{Mms1/Mms22}$ is similar to the mammalian $Cul4^{Ddb1}$ complex (Zaidi *et al.*, 2008). $Cul4^{Ddb1}$ is a ubiquitin ligase with a number of roles in genome maintenance (for a review see Jackson and Xiong, 2009), including degradation of the replication factors CDT1 and CHK1 (Higa *et al.*, 2003; Leung-Pineda *et al.*, 2009) and ubiquitination of histones and XPC under conditions of DNA damage (Sugasawa *et al.*, 2005; Kapetanaki *et al.*, 2006; Wang *et al.*, 2006). As is the case for the $Cul4^{Ddb1}$ ubiquitin ligase, $Rtt101^{Mms1}$ forms multiple complexes with several substrate specific adaptors, and these are expected to dictate function (Zaidi *et al.*, 2008; Fujii *et al.*, 2009; Mimura *et al.*, 2010).

The precise role for this $Cul4^{Ddb1}$-like complex, $Rtt101^{Mms1/Mms22}$, in maintaining genome integrity in response to replication stress has yet to be determined. Here we show that Mms1 localizes to regions adjacent to replication origins when replication stress is present, suggesting that Mms1 is recruited to stalled replication forks. We find that deletion of *MMS1* or *MMS22* reduces the association of replisome proteins with stalled replication forks, and that, in the absence of *MMS1* or *MMS22* replication forks progress and recover inefficiently in the presence of HU. Together our results indicate that Mms1 and Mms22 are important for the stabilization of protein components at the replication fork during replication stress and thereby function to prevent fork collapse and promote the resumption of DNA synthesis.

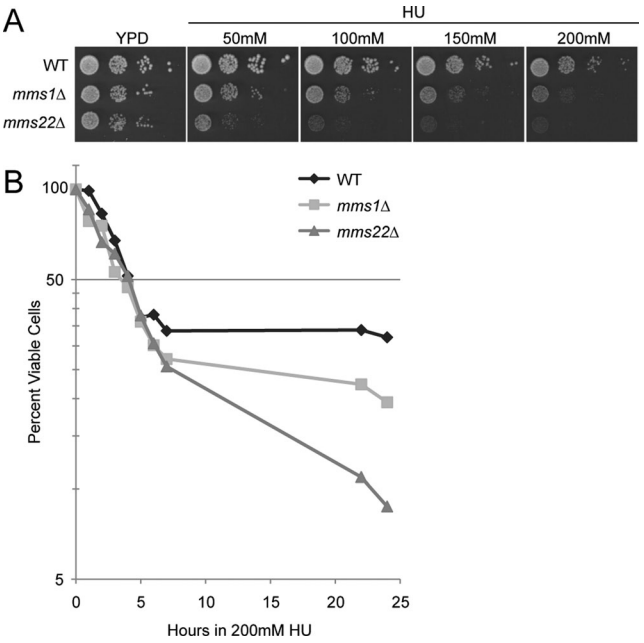

FIGURE 1: Mms1 and Mms22 are important for viability in the presence of replication stress. (A) Tenfold serial dilutions of wild-type, *mms1*Δ, and *mms22*Δ strains were spotted on YPD containing 0, 50, 100, 150, or 200 mM HU. Plates were incubated at 30°C for 2–3 d. (B) Wild-type, *mms1*Δ, and *mms22*Δ cells in early log phase were treated with 200 mM HU. Samples were collected at the indicated time points and plated on YPD to determine the number of colony-forming units. The average of two independent experiments is plotted.

RESULTS

Deletion of *MMS1* or *MMS22* causes an abnormal cell cycle following recovery from replication stress

Deletion of *MMS1* or *MMS22* renders cells sensitive to DNA-damaging agents (Bennett *et al.*, 2001; Chang *et al.*, 2002; Hryciw *et al.*, 2002; Araki *et al.*, 2003; Baldwin *et al.*, 2005; Dovey and Russell, 2007; Dovey *et al.*, 2009; Yokoyama *et al.*, 2007; Roberts *et al.*, 2008) and to replication stress caused by chronic exposure to HU (Chang *et al.*, 2002; Araki *et al.*, 2003; Dovey and Russell, 2007; Dovey *et al.*, 2009; Yokoyama *et al.*, 2007; Roberts *et al.*, 2008) (Figure 1A). To delineate the role of *MMS1* and *MMS22* in HU resistance, we assessed the viability of *mms1*Δ and *mms22*Δ over a 24 h period of HU exposure (Figure 1B). Samples were collected at the indicated times from wild-type, *mms1*Δ, and *mms22*Δ cultures treated with 200 mM HU, and viability was measured following plating on media lacking HU. Replication stress began to affect viability in *mms1*Δ and *mms22*Δ after 6 h of HU treatment, indicating that even during short-term exposure Mms1 and Mms22 are required for HU resistance. Consistent with previous assays of MMS sensitivity, *mms22*Δ was more sensitive to HU than was *mms1*Δ (Roberts *et al.*, 2008; Zaidi *et al.*, 2008; Dovey *et al.*, 2009).

We next examined cell cycle progression in *mms1*Δ and *mms22*Δ strains during treatment with HU for 90 min, and during a subsequent 3 h recovery period, by flow cytometry and by

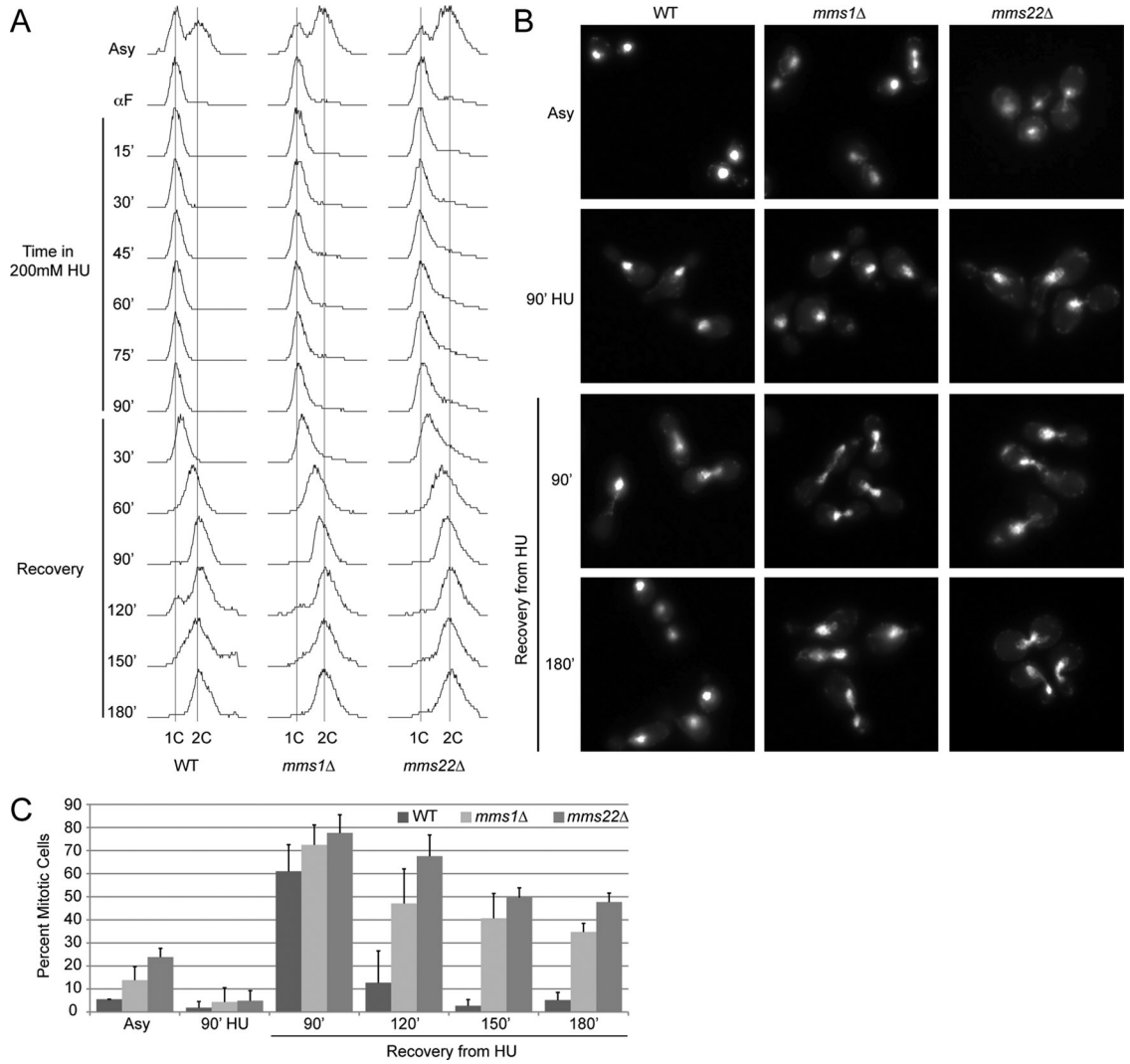

FIGURE 2: *mms1*Δ and *mms22*Δ cells exhibit cell cycle defects during recovery from replication stress. Asynchronously growing cultures (Asy) were arrested in G1 with α-factor (αF), released into 200 mM HU for 90 min, and then washed and released into YPD for 3 h. Samples were collected every 30 min. (A) Flow cytometric analysis of DNA contents. Positions of cells with 1C and 2C DNA contents are indicated. (B) Fluorescence micrographs of fixed cells stained with DAPI to visualize nuclear morphology during HU treatment and subsequent recovery. (C) Large-budded cells with DNA spanning the bud neck were quantified at the indicated times.

examination of cell morphology (Figure 2). Wild-type, *mms1*Δ, and *mms22*Δ strains progress similarly during the HU treatment, arresting early in S phase (Figure 2A). On removal of HU and release into fresh media, the wild-type strain progresses through the cell cycle and completes mitosis within 2 h, as evidenced by the reemergence of cells with 1C DNA contents (Figure 2A, 120 min) and by the decrease in mitotic cells (Figure 2, B and C). By contrast, *mms1*Δ and *mms22*Δ strains remain with 2C DNA contents and do not complete mitosis within 3 h, suggesting that proper and timely recovery from HU-induced replication fork stalling requires Mms1 and Mms22. In addition, we noted that during recovery from HU the *mms1*Δ and *mms22*Δ strains accumulated with a distinct morphology (Figure 2B). The mutant cells accumulated as large, budded cells with the nuclear DNA spanning the bud neck. This nuclear morphology is similar to that seen during recovery of *mms1*Δ and *mms22*Δ cells from MMS damage (Duro *et al.*, 2008) and is reminiscent of mutants that attempt mitosis with unreplicated regions (Torres-Rosell *et al.*, 2007).

Deletion of *MMS1* results in abnormal replication fork progression during replication stress

The lengthy mitotic delay in *mms1*Δ and *mms22*Δ strains following replication stress suggested that DNA replication in the absence of Mms1 or Mms22 might be defective when HU-induced replication stress is present. We examined replication dynamics in wild-type and *mms1*Δ strains in the presence of replication stress. G1-arrested cells were released into media containing both bromodeoxyuridine (BrdU), to label newly synthesized DNA, and HU, to stall replication. The wild-type and *mms1*Δ cultures were sampled at 45 and 90 min, and BrdU-labeled DNA was hybridized to tiling microarrays to identify replicated regions genome wide. The wild-type strain exhibited narrow peaks of BrdU incorporation at early-firing replication origins after 45 min in HU (Figure 3A, top). These peaks broadened after 90 min (Figure 3A, bottom), consistent with the observation that HU slows, but does not arrest, DNA synthesis in wild-type cells (Alvino *et al.*, 2007). By contrast, DNA synthesis in *mms1*Δ cells was defective in several ways. First, the BrdU peaks were broader at 45 min when compared with wild-type cells (Figure 3B, top), indicating that

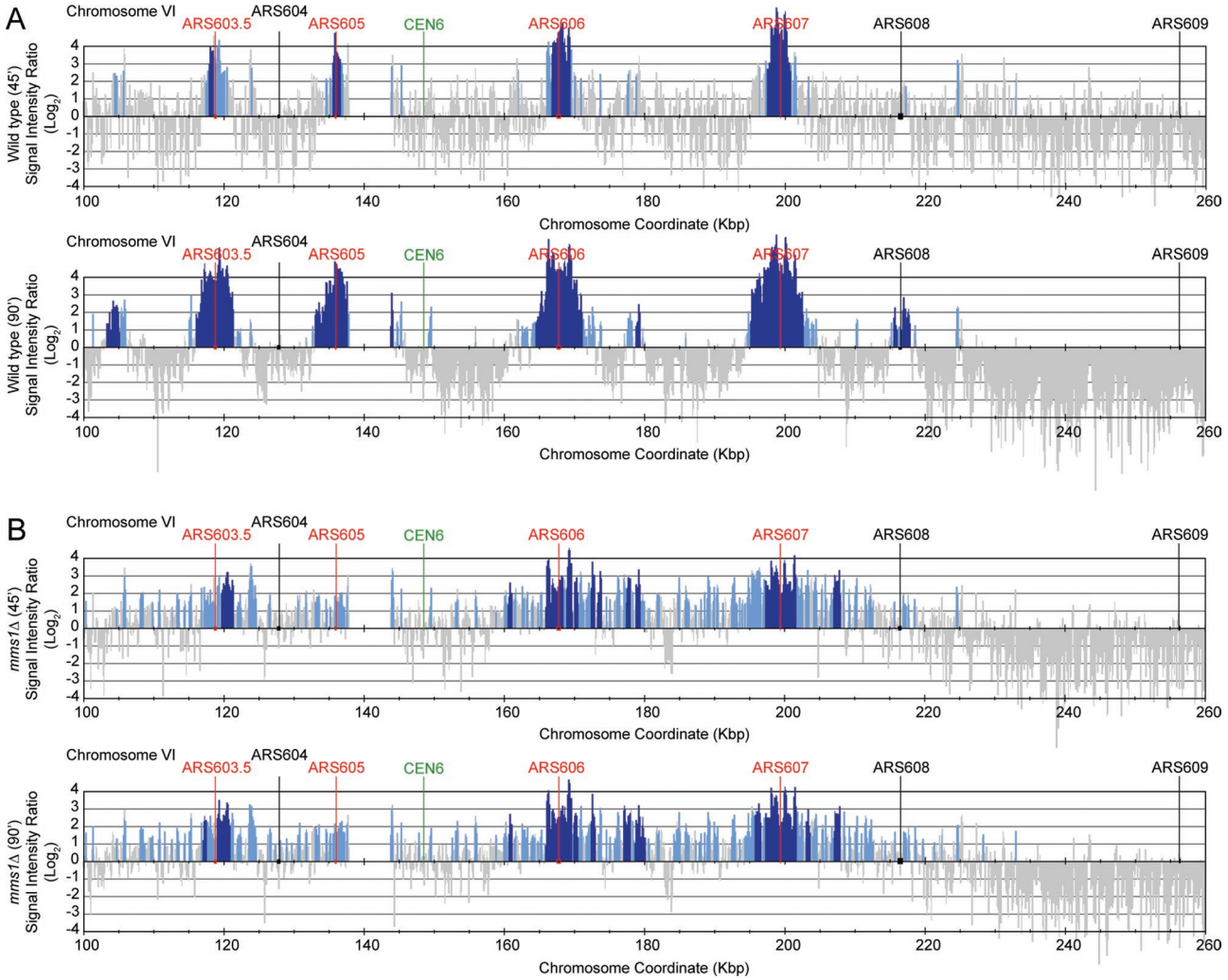

FIGURE 3: *mms1*Δ cells have an irregular pattern of fork progression in HU. BrdU IP-chip analysis was performed following synchronous release of wild-type (A) and *mms1*Δ (B) strains into 200 mM HU for 45 min (top) or 90 min (bottom). Enrichment of DNA fragments in the BrdU sample relative to an unreplicated control is shown along chromosome VI. The signal intensity ratio on a $\log_2$ scale is shown on the *y*-axis and the chromosome coordinate is shown on the *x*-axis. Positive signal represents regions that are replicated, and regions where the positive signal is statistically significant over 300 base pairs are shown in light blue and over 900 base pairs are shown in dark blue. Replication origins (ARSs) are indicated. Early-firing origins are colored red.

replication forks traveled further in the mutant relative to wild type when replication stress was present. Second, the BrdU peak height at 45 min was reduced in *mms1*Δ compared with wild type, which might indicate greater variation in the distances traveled by individual replication forks in the population. Third, the BrdU peaks in *mms1*Δ cells were largely unchanged at 90 min (Figure 3B, bottom), suggesting the absence of significant DNA replication in the mutant between 45 and 90 min. We conclude that DNA synthesis during replication stress in *mms1*Δ is initially advanced but then halts as replication forks arrest. We were unable to analyze replication in *mms22*Δ mutants, as deletion of *mms22* in the multicopy thymidine kinase strain that allows incorporation of BrdU resulted in a synthetic sick phenotype (unpublished data).

Mms1 binds origin-proximal regions when replication forks stall

Several studies have suggested that Mms1 and Mms22 function to maintain the stability of the genome (Bennett *et al.*, 2001; Chang *et al.*, 2002; Hryciw *et al.*, 2002; Araki *et al.*, 2003; Baldwin *et al.*, 2005; Dovey and Russell, 2007; Dovey *et al.*, 2009; Yokoyama *et al.*, 2007; Duro *et al.*, 2008; Roberts *et al.*, 2008; Zaidi *et al.*, 2008; Ben-Aroya *et al.*, 2010; Mimura *et al.*, 2010); however, it remains unclear how they exert this effect. Our data indicated that absence of Mms1 caused defects in DNA replication when replication fork stress was present, suggesting that Mms1 might act directly at stalled replication forks. We examined the association of Mms1 with sites of stalled replication forks using chromatin immunoprecipitation (ChIP) (Figure 4, A–C). Cells were arrested in G1 phase and released into S phase in the presence of HU. Following cross-linking to preserve protein–DNA interactions, Mms1–DNA complexes were isolated, and the enrichment of an early-firing origin of replication, ARS607, versus that of a late-firing origin, ARS609, was measured using quantitative PCR (qPCR). We observed a twofold enrichment at the early-firing replication origin in the Mms1 immunoprecipitate relative to the late-firing origin, which is dormant in HU. A similar result was found when we compared enrichment of an active origin (ARS1018) with an interorigin region between ARS1009 and ARS1010 that lacks active replication origins (Figure 4A). Together,

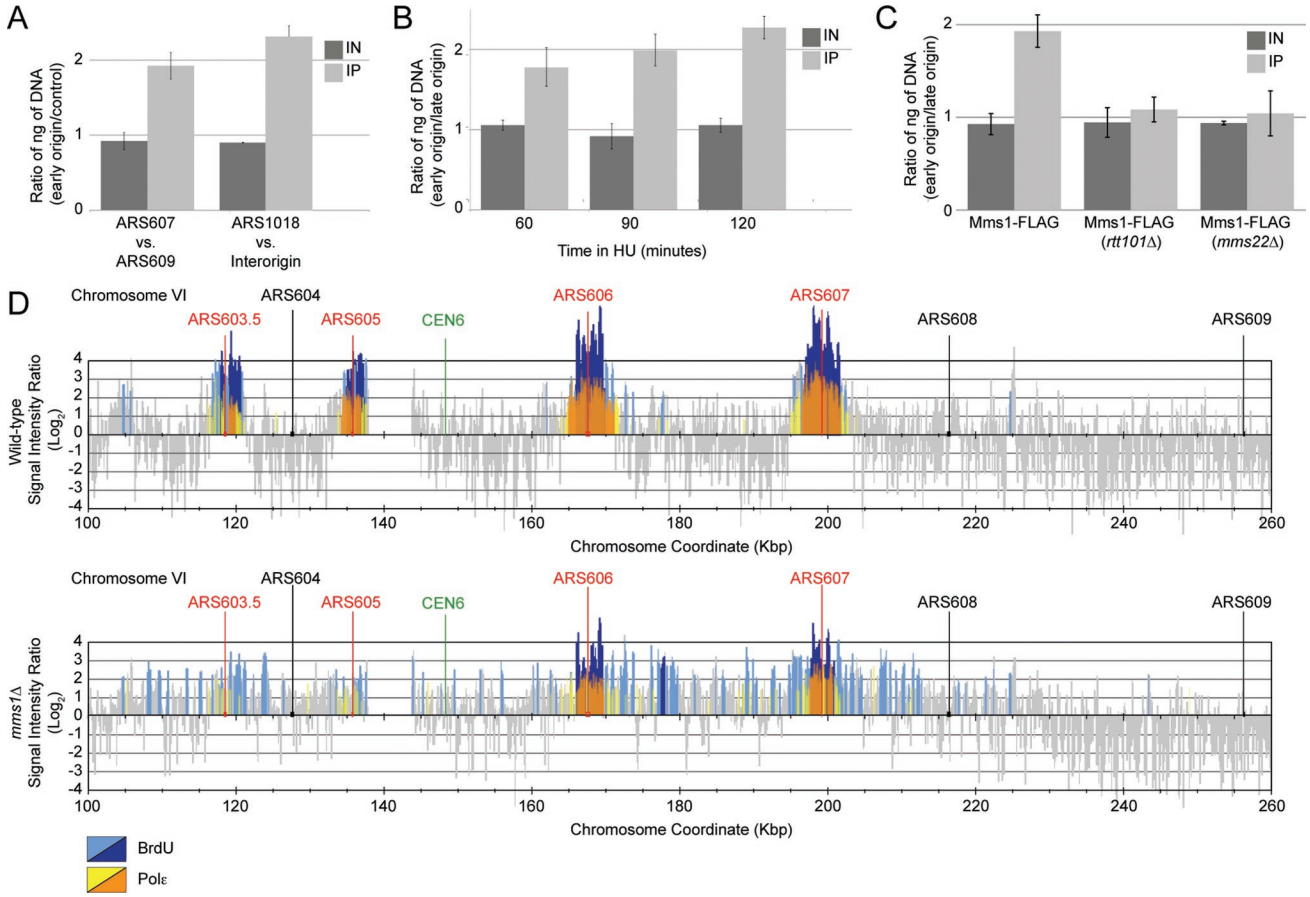

FIGURE 4: Mms1 binds to origin-proximal regions when replication forks stall and is important for replisome stability at stalled forks. (A–C) ChIP analysis of Mms1-FLAG in the indicated strain backgrounds was performed following synchronous release of cells into S phase in the presence of 200 mM HU for 90 min at 23°C. Enrichment of early-origin DNA fragments relative to late-origin DNA in the Mms1-bound and input fractions was measured by quantitative PCR. The average of at least two experiments is plotted, and the SD is shown. (A) ChIP analysis of Mms1 localization to two early-firing origins of replication. Mms1 association with DNA was analyzed by calculating the ratio of early-origin DNA (ARS607 or ARS1018) to late-origin DNA (ARS609) or DNA associated with an interorigin region (between ARS1009 and ARS1010). (B) Time course of Mms1 localization to origin-proximal regions (ARS607 vs. ARS609). Samples were collected at the indicated time points and processed for ChIP/qPCR. (C) ChIP/qPCR of Mms1 in *RTT101* and *MMS22* mutants (ARS607 vs. ARS609). (D) ChIP-chip was performed in parallel with BrdU IP-chip following synchronous release of *DPB3::flag* cells into S phase in the presence of 200 mM HU for 90 min at 23°C. Enrichment of DNA fragments in the BrdU sample relative to an unreplicated control and enrichment of DNA fragments in the Dpb3-bound fraction relative to the unbound fraction are shown along chromosome VI. The signal intensity ratio on a $\log_2$ scale is shown on the *y*-axis and the chromosome coordinate is shown on the *x*-axis. Positive signal (blue) represents regions that are replicated, and regions where the positive signal is statistically significant over 300 base pairs are shown in light blue and over 900 base pairs are shown in dark blue. Positive signal (yellow/orange) represents occupancy by Dpb3, and regions where the positive signal is statistically significant (Katou *et al.*, 2006) over 300 base pairs are shown in yellow and over 900 base pairs are shown in orange. Replication origins (ARSs) are indicated in red for early-firing origins that are active in HU and in black for late-firing origins that are inactive in HU.

these data indicate that Mms1 associates with early-firing origins of replication when replication forks stall. We next looked at Mms1 dynamics by conducting an Mms1 ChIP/qPCR time course with the ARS607/ARS609 probe pair. If Mms1 functions at replication forks, the levels of Mms1 protein detected at these sites may change with time as forks accumulate at the probe region. We detected a modest but significant increase in the amount of early-origin DNA in Mms1 immunoprecipitates between 60 and 120 min (Figure 4B).

Mms1 functions as part of a complex with Rtt101 and Mms22 (Zaidi *et al.*, 2008; Mimura *et al.*, 2010). We examined whether binding of Mms1 at stalled replication forks required either of the Mms1-binding partners. Using ChIP/qPCR, we found that enrichment of the early-origin DNA in Mms1 chromatin immunoprecipitates was abolished in *rtt101*Δ and in *mms22*Δ strains (Figure 4C). Thus the presence of Mms1 at an active replication origin when replication stress is present depends on the known Mms1-binding partners Mms22 and Rtt101.

Because DNA synthesis is defective in *mms1*Δ strains during replication fork stress and Mms1 associates with replication forks, we performed parallel BrdU immunoprecipitation (IP)-chip and ChIP-chip experiments to examine the localization of fork proteins during DNA replication in *mms1* mutants (Figure 4D). We tagged Dpb3, a subunit of DNA polymerase epsilon (Polε), in wild-type and *mms1*Δ strains to assess protein–DNA association and DNA synthesis concurrently. As the leading-strand polymerase, Polε localizes to origins of replication and colocalizes with sites of DNA synthesis (Aparicio

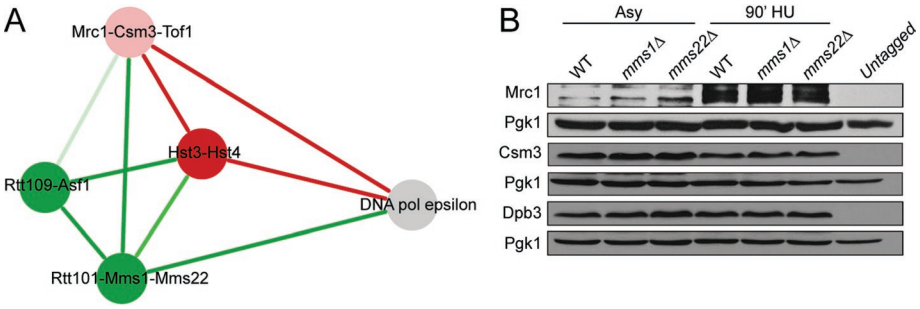

FIGURE 5: Genetic interactions suggest that Mms1 and Mms22 function with components of the replisome. (A) Genetic interaction map of the Rtt101-Mms1-Mms22 complex. The genetic interactions of *MMS1*, *MMS22*, and *RTT101* and genes encoding components of the indicated protein complexes were compiled from high-throughput SGA experiments. Genetic interactions were determined both within and between protein complexes. Complexes are displayed as colored nodes: green when interactions between members are positive, red when interactions between members are negative, and gray when the complex includes an essential component. Nodes are connected by green lines when the between-complex interactions are positive and by red lines when the between-complex interactions are negative. (B) Western blot analysis of the indicated strains. Denatured extracts were prepared from asynchronously growing cultures (Asy) and after 90 min in 200 mM HU (90′ HU). Antibodies directed against the FLAG epitope fused to Mrc1, Csm3, and Dpb3 and against phosphoglycerate kinase (loading control) were used to detect each protein.

et al., 1997; Hiraga *et al.*, 2005; Lou *et al.*, 2008). Strains were blocked in G1 and released into media containing HU to induce replication fork stress and BrdU to label newly synthesized DNA. In the wild-type strain, treatment with HU for 90 min results in overlapping BrdU and Dpb3 signals, with both peaks restricted to regions surrounding early-firing origins of replication. Remarkably, although the profile of BrdU incorporation in the *mms1*Δ strain shows a broader distribution than in the wild-type strain, Dpb3 localizes to the same chromosome coordinates as in the wild type and does not colocalize with the BrdU signal. This suggests that in *mms1*Δ, forks that are more distal from the origin no longer have Dpb3 (Polε) associated with them. This is consistent with the data in Figure 3, which indicate little change in the sites of DNA synthesis in *mms1*Δ between 45 and 90 min. We conclude that the replisome or replisome components have dissociated from these forks and that these forks are no longer synthesizing DNA.

Mms1 and Mms22 stabilize replication proteins at stalled replication forks

Our data indicate that replication forks arrest in *mms1*Δ and *mms22*Δ cells in the presence of replication stress and that replication does not resume efficiently during recovery from replication stress. Furthermore, our data suggest that replication fork proteins likely dissociate from forks in the absence of Mms1 or Mms22. We mined high-throughput genetic interaction data sets to identify candidate genes whose function might be influenced by the absence of *mms1*, *mms22*, and *rtt101* (Costanzo *et al.*, 2010; Koh *et al.*, 2010). The genes encoding members of the Rtt101$^{Mms1/Mms22}$ complex exhibited positive genetic interactions with genes encoding proteins that reside at the replication fork, including Mrc1, Csm3, and Tof1, and DNA Polε (Figure 5A). Mrc1-Csm3-Tof1 form a replication fork–pausing complex (FPC) that tethers the MCM helicase to the leading-strand polymerase, Polε, when forks are stalled (Katou *et al.*, 2003; Calzada *et al.*, 2005; Nedelcheva *et al.*, 2005; Szyjka *et al.*, 2005; Lou *et al.*, 2008). Although positive interactions often connect members of the same nonessential complex, analysis of genetic interaction networks showed that the vast majority of positive interactions occur between different protein complexes, which may belong to a common biological pathway (Baryshnikova *et al.*, 2010; Costanzo *et al.*, 2010). Thus these data suggest that the fork-pausing complex or the leading-strand polymerase may be targets of Rtt101$^{Mms1/Mms22}$ action.

We assessed whether deletion of *MMS1* or *MMS22* altered the association of the FPC with forks when replication stress is applied. Steady-state levels of the replication fork proteins Mrc1, Csm3, and Dpb3 were not reduced by deletion of either *MMS1* or *MMS22*, indicating that any observed effects were not due to decreased protein abundance (Figure 5B). We examined the recruitment of Mrc1 to stalled forks genome wide by ChIP-chip in wild-type, *mms1*Δ, and *mms22*Δ strains (Figure 6, A and B). As reported, Mrc1 localizes to origin proximal regions in HU-treated cells (Katou *et al.*, 2003). However in *mms1*Δ and *mms22*Δ strains, the enrichment of origin proximal regions was decreased (Figure 6, A and B, bottom). Although the signal intensity ratio was lower in the mutants, Mrc1 localization occurred at the same chromosome coordinates, suggesting that there is less Mrc1 at these sites and not a spreading of Mrc1 to adjacent regions. This effect was observed genome wide in both *mms1*Δ and *mms22*Δ mutants. Consistent with our HU sensitivity data, according to which *mms22*Δ mutants display a more severe growth defect under conditions of replication stress than *mms1*Δ mutants, deletion of *MMS1* had a more subtle effect on Mrc1 localization than deletion of *MMS22*. To corroborate this finding, we analyzed the signal intensity peak areas at 12 early-firing origins of replication and compared the distribution in wild-type to that in *mms1*Δ and *mms22*Δ strains. The median peak area for Mrc1 was significantly decreased ($p < 0.05$) in *mms1*Δ and *mms22*Δ strains compared with their respective wild-type controls (Figure 6C). Again, this effect was stronger in the *mms22*Δ strain. Together, the ChIP-chip data indicate that deletion of *MMS1* or *MMS22* reduces Mrc1 localization to stalled replication forks under conditions of fork stress. We quantified the reduction in Mrc1 localization to replication origins using qPCR to measure enrichment of the early-firing origin ARS607 compared with the inactive (in HU) origin ARS609 in at least two independent Mrc1 chromatin immunoprecipitates from each of the wild-type, *mms1*Δ, and *mms22*Δ strains. The enrichment of the early-firing origin in the Mrc1 immunoprecipitates was reduced to approximately half of the wild-type level in both the *mms1*Δ and the *mms22*Δ mutants (Figure 6D). To confirm that this effect is not unique to Mrc1, we examined the localization of Csm3, a second component of the fork-pausing complex, to these same chromosome coordinates by qPCR. Similar to Mrc1, *mms1*Δ and *mms22*Δ strains exhibit a twofold reduction in early origin enrichment in the Csm3 immunoprecipitates (Figure 6E). These data indicate that Mms1 and Mms22 promote the stable binding of the FPC at replication forks under conditions of replication fork stress.

Given that Mrc1 links Polε to the replicative helicase when forks stall (Lou *et al.*, 2008), and since Polε exhibits positive genetic interactions with the Rtt101-Mms1-Mms22 pathway/complex, we assessed the association of Dpb3, a subunit of DNA Polε, with stalled forks. Deletion of *MMS1* or *MMS22* resulted in a significant reduction in the amount of Dpb3 at early-firing origins, genome wide, by ChIP-chip (Figure 7, A–C). As was observed for Mrc1, deletion of

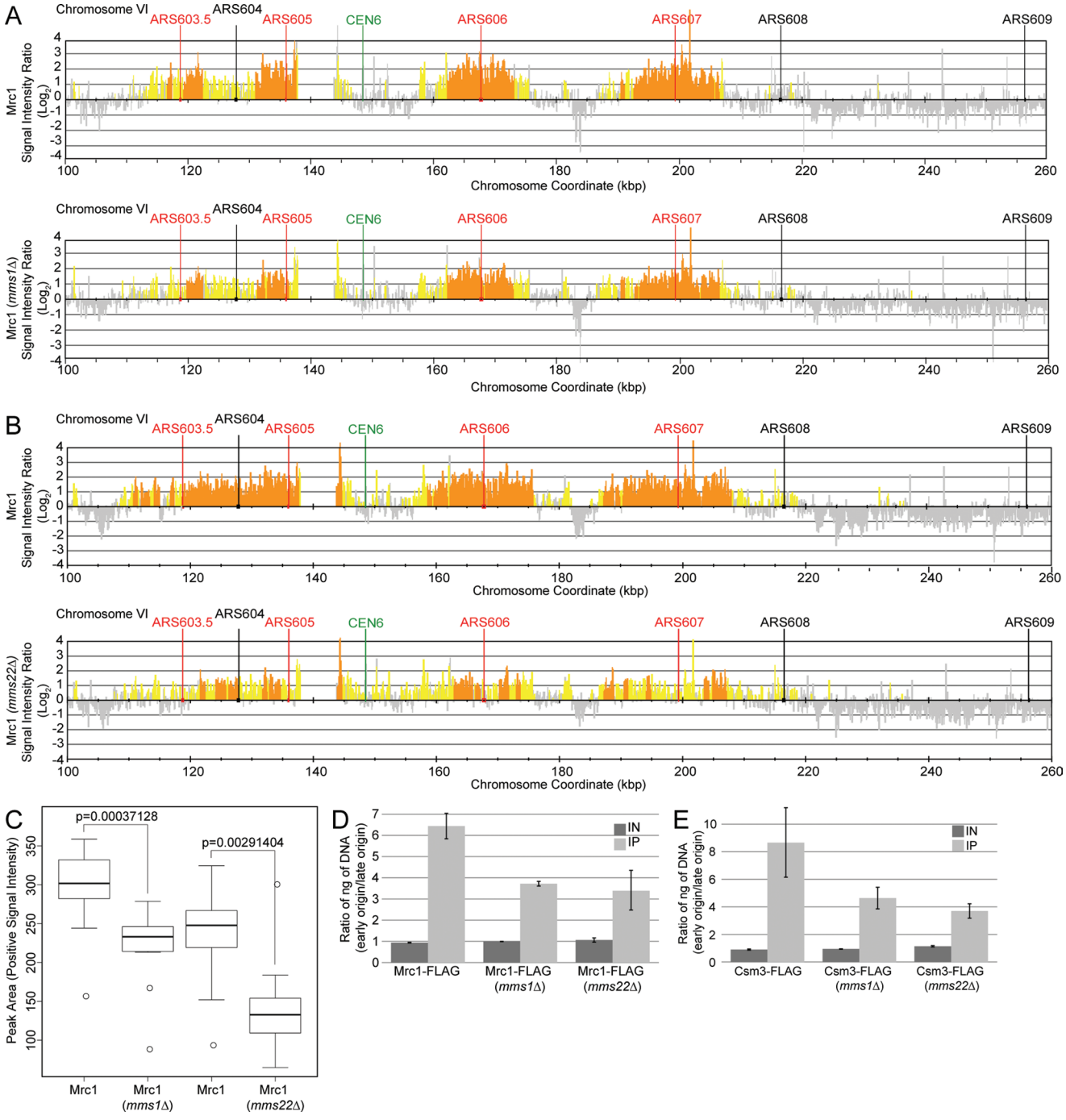

FIGURE 6: Deletion of *MMS1* or *MMS22* reduces the association of the FPC with stalled replication forks. (A, B) ChIP-chip analysis was performed following synchronous release of *MRC1::flag*, *mms1Δ MRC1::flag*, or *mms22Δ MRC1::flag* cells into S phase in the presence of 200 mM HU for 90 min at 23°C. After cross-linking and DNA fragmentation, Mrc1 was precipitated. Enrichment of DNA fragments in the Mrc1-bound fraction relative to the unbound fraction is shown along chromosome VI, as in Figure 4D. Replication origins (ARSs) are indicated in red for early-firing origins that are active in HU and in black for late-firing origins that are inactive in HU. (C) The distributions of signal intensity peak areas in the ChIP-chip data for 12 replication origins for the indicated strains is shown as a boxplot, with the median indicated by the horizontal bar. Peak areas were determined by extracting the signal intensity ratio values plotted in A and B at 50-nucleotide (nt) intervals for 5000 nt on either side of each origin and summing those values. Significant differences in distributions between each mutant and its wild-type control as calculated using a Mann–Whitney test are indicated. (D) Enrichment of early-origin DNA fragments relative to late-origin DNA in the Mrc1-bound and input fractions was quantified by quantitative PCR for the indicated strains. The ratio of early-origin DNA (ARS607) to late-origin DNA (ARS609) was quantified for the input and the Mrc1-bound fractions. The average of at least two experiments is plotted, and the SD is shown. (E) Enrichment of DNA fragments in the Csm3-bound fraction from chromatin immunoprecipitations of wild-type, *mms1Δ*, and *mms22Δ* strains was quantified by quantitative PCR. The ratio of early-origin DNA (ARS607) to late-origin DNA (ARS609) was quantified for the input and the Csm3-bound fractions. The average of at least two experiments is plotted, and the SD is shown.

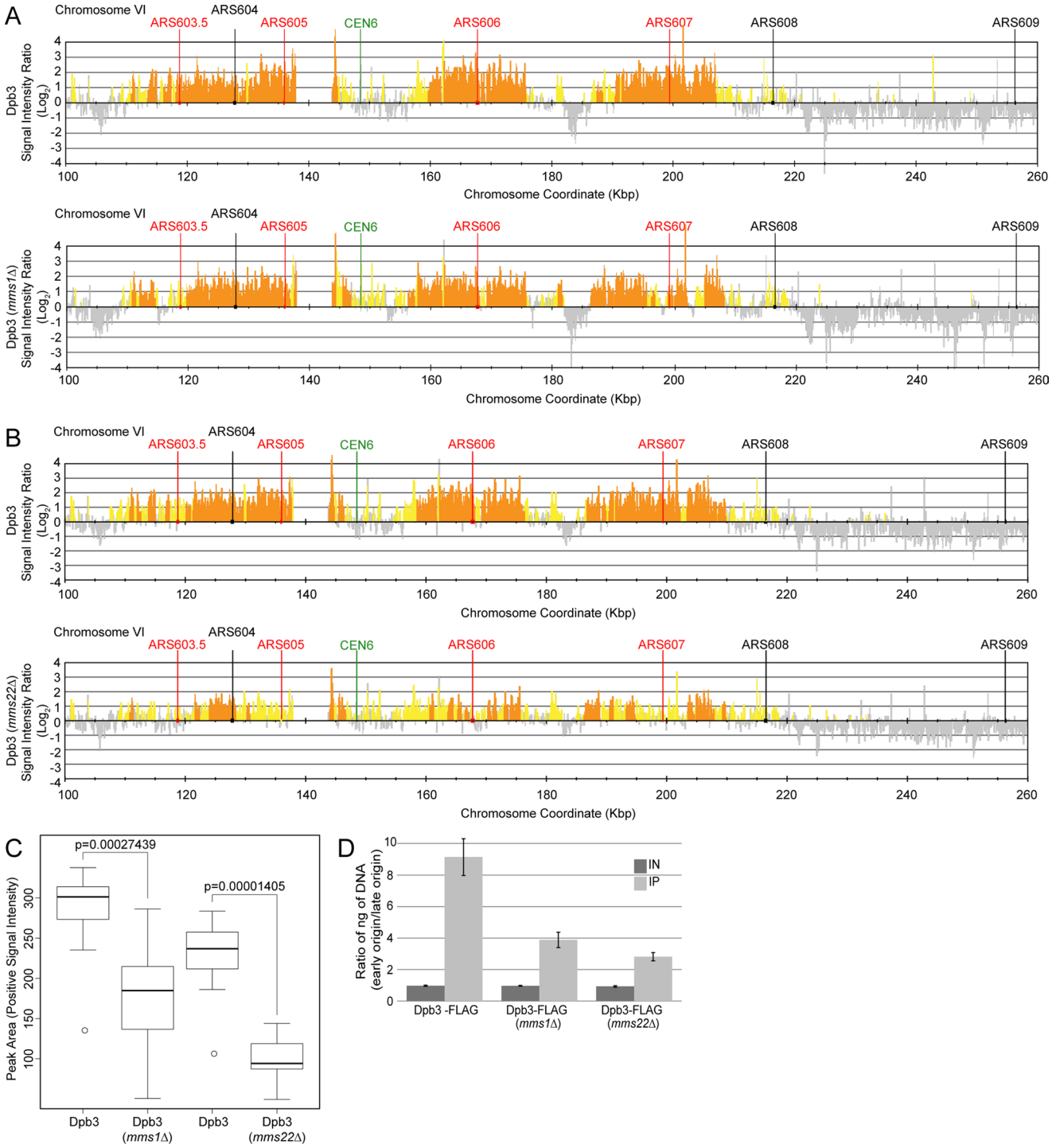

FIGURE 7: Deletion of *MMS1* or *MMS22* reduces the association of DNA Polε with stalled replication forks. (A, B) ChIP-chip analysis was performed following synchronous release of *DPB3::flag*, *mms1Δ DPB3::flag*, or *mms22Δ DPB3::flag* cells into S phase in the presence of 200 mM HU for 90 min at 23°C. After cross-linking and DNA fragmentation, Dpb3 was precipitated. Enrichment of DNA fragments in the Dpb3-bound fraction relative to the unbound fraction is shown along chromosome VI, as in Figure 4D. Replication origins (ARSs) are indicated in red for early-firing origins that are active in HU and in black for late-firing origins that are inactive in HU. (C) The distributions of signal intensity peak areas in the ChIP-chip data for 12 replication origins for the indicated strains is shown as a boxplot, with the median indicated by the horizontal bar. Peak areas were determined by extracting the signal intensity ratio values plotted in A and B at 50-nt intervals for 5000 nt on either side of each origin and summing those values. Significant differences in distributions between each mutant and its wild-type control as calculated using a Mann–Whitney test are indicated. (D) Enrichment of early-origin DNA fragments relative to late-origin DNA from the Dpb3-bound and input fractions was quantified by quantitative PCR for the indicated strains. The ratio of early-origin DNA (ARS607) to late-origin DNA (ARS609) was quantified for the input and the Dpb3-bound fractions. The average of at least two experiments is plotted, and the SD is shown.

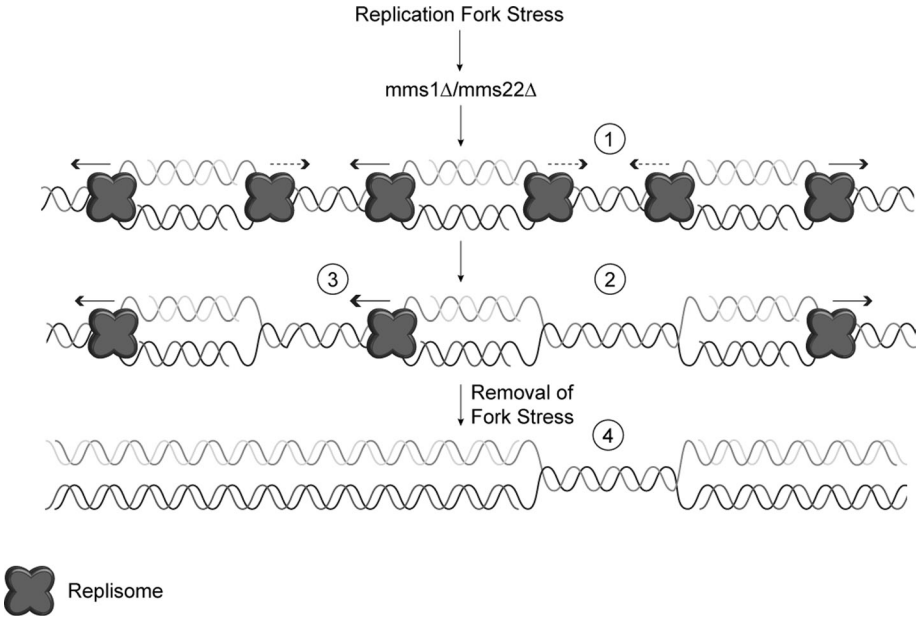

FIGURE 8: Mms1 and Mms22 stabilize the replisome when replication forks stall. In wild-type cells Mms1 and Mms22, either alone or as part of the $Rtt101^{Mms1/Mms22}$ complex, are important for the stable association of the replisome with replication forks during replication stress. In *mms1*Δ or *mms22*Δ strains, the decrease in the association of key replisome components with replication forks results in defects in DNA replication. Under conditions of replication stress, the replisome must be stabilized at stalled forks (1). In *mms1*Δ/*mms22*Δ strains, this stabilization is reduced at a subset of replication forks (dotted arrows), causing replisome components to dissociate (2). This effect is confined to a subset of replication origins, leaving some intact forks to resume synthesis once the HU has been removed (3). At many sites, loss of an intact replisome at an origin will be compensated for by a neighboring origin. However, rare regions flanked by collapsed forks will remain unreplicated (4), resulting in mitotic delay, genomic instability, and loss of viability.

MMS22 had a more pronounced effect on Dpb3 localization than *MMS1* deletion. We quantified this reduction by qPCR and found that strains carrying deletions of *MMS1* or *MMS22* had a greater-than-twofold reduction in Dpb3 localization to early-firing origins of replication (Figure 7D).

Together, these data indicate that Mms1 and Mms22 are important for the stable association of the fork-pausing complex (Mrc1/Tof1/Csm3) and the leading-strand polymerase with the replisome when replication stress is present. The consequence of the partial dissociation of these factors is fork arrest in the presence of replication stress, mitotic defects during recovery from replication stress, and loss of viability.

DISCUSSION

We have characterized the function of *MMS1* and *MMS22* during replication stress induced by HU. Following short-term exposure to HU, *mms1*Δ and *mms22*Δ strains have decreased viability and are unable to complete mitosis efficiently, accumulating with an anaphase-like morphology. DNA replication in the *mms1*Δ mutant is defective, and replication forks stall in the presence of replication stress. Finally, we find that the association of replisome components with the stressed replication forks decreases by twofold. Together our data suggest a model in which the function of Mms1, and perhaps Mms22, is to promote the stable association of the fork-pausing complex, the leading-strand polymerase, and likely other replisome components with the replication fork when replication stress is present. In the absence of Mms1 (and by extension Mms22) the dissociation of fork components results in replication fork stalling and perhaps collapse, leading to inefficient DNA synthesis during recovery from replication stress (Figure 8).

DNA synthesis in the presence of replication stress is perturbed in *mms1*Δ and *mms22*Δ cells

Our data show that DNA synthesis at replication forks in the presence of HU is defective in *mms1*Δ mutants. Unexpectedly, *mms1*Δ displayed broader replication peaks than did the wild-type strain after 45 min in HU. Because the replication peaks were shallower than in wild type and there was little difference evident in the flow cytometry profiles, we infer that there is considerable diversity in the amount of DNA synthesis at individual replication forks in individual cells in the population analyzed. This could reflect some degree of HU-resistant DNA synthesis, as we have observed in mutants in *elg1* and *pol30* (M.B. Davidson, Y. Katou, A. Keszthelyi, J. Ou, T.L. Sing, J.A. Vaisica, A. Chabes, K. Shirahige, and G.W. Brown, unpublished data), or an asynchronous or advanced entry into S phase in *mms1*Δ. A similar advanced DNA synthesis in HU was seen in *ctf18*Δ mutants, although in contrast to *mms1*Δ this was accompanied by checkpoint activation defects (Crabbe *et al.*, 2010). Despite this initial burst of DNA synthesis, *mms1*Δ showed little change in replication peaks between 45 and 90 min, suggesting that forks had completely arrested. This contrasts with wild-type cells, which continue to synthesize DNA in the presence of HU but at lower rates (Figure 3) (Alvino *et al.*, 2007). Furthermore, in *mms1*Δ strains, we found that Polε does not colocalize with the BrdU signal after 90 min in HU, and in particular origin-distal forks appear to lack Polε (Figure 4D). Given the replication profile of the mutant, we suggest that during replication fork stress in *mms1*Δ strains, replication at a subset of origins initially proceeds more rapidly than in wild type, resulting in DNA synthesis at more origin-distal sites. These forks ultimately arrest and lose replisome components, failing to synthesize DNA after 45 min in HU (Figure 8). Consistent with the arrest and/or collapse of a subset of replication forks in HU in *mms1*Δ, we found that completion of S phase remained defective in the mutant even after the removal of HU, as evidenced by the persistence of mitotic forms in the mutant. Together our data are consistent with a loss of replisome integrity in *mms1*Δ.

Mms1 and Mms22 are important for the stabilization of the replisome during replication stress

We find that Mms1 and Mms22 are important mediators of Mrc1 localization to sites of stalled replication. Under conditions of replication stress, checkpoint activation is modulated by the phosphorylation of the mediator protein Mrc1 (Alcasabas *et al.*, 2001; Naylor *et al.*, 2009). In addition to its role in checkpoint signaling, Mrc1 is present at replication forks and forms a complex with Csm3 and Tof1 called the FPC (Katou *et al.*, 2003;

Osborn and Elledge, 2003; Noguchi *et al.*, 2004; Calzada *et al.*, 2005; Nedelcheva *et al.*, 2005; Szyjka *et al.*, 2005; Lou *et al.*, 2008; Bando *et al.*, 2009; Shimmoto *et al.*, 2009). FPC function is critical not only under conditions of fork stress, but also during a normal, unperturbed cell cycle (Tourriere *et al.*, 2005; Lou *et al.*, 2008). Our data reveal that localization of Mrc1 and Csm3 is decreased twofold in *mms1*Δ and *mms22*Δ strains, suggesting that one role of Mms1 and Mms22 is to stabilize the FPC component of the replisome under conditions of replication stress. As a component of the FPC, Mrc1 tethers the leading-strand polymerase, Polε, to the replicative MCM helicase until DNA synthesis can safely resume (Lou *et al.*, 2008). We examined the enrichment of Dpb3, a nonessential subunit of Polε, and found that it too was decreased by at least twofold. By both ChIP-chip and ChIP/qPCR, deletion of *MMS22* was found to have a more prominent effect on localization of fork proteins than deletion of *MMS1* under conditions of replication fork stress. This is consistent with our data demonstrating that *mms22*Δ mutants are more sensitive to HU than are *mms1*Δ strains. Likewise, we and others have previously demonstrated that *mms22*Δ is more sensitive than *mms1*Δ to the DNA-alkylating agent MMS (Roberts *et al.*, 2008; Zaidi *et al.*, 2008; Dovey *et al.*, 2009). Although the basis for this increased sensitivity is unknown, *mms1*Δ *mms22*Δ double mutants are no more sensitive than *mms22*Δ in their sensitivity to HU or MMS (unpublished data), suggesting that Mms22 has roles independent of Mms1 under conditions of replication stress and DNA damage.

The effects of *MMS1* and *MMS22* deletion are likely not restricted to the FPC and Polε. Like the tethering effect of Mrc1 on Polε, Ctf4 binds and regulates Polα (Gambus *et al.*, 2009; Tanaka *et al.*, 2009), and Rtt101-Mms1-Mms22 binds Ctf4 (Mimura *et al.*, 2010), indicating that Mms1 and Mms22 could modulate DNA Polα association with the replisome. Furthermore, *RTT101*, *MMS1*, and *MMS22* have highly correlated genetic interactions with *CTF4*, suggesting that they may function in concert (C. Boone, unpublished data). The $Rtt101^{Mms1/Mms22}$ complex could stabilize stalled replication forks by interacting with both the leading and lagging strands of forks via Ctf4 and Mrc1. Consistent with Mms1 and Mms22 promoting replisome stability during replication stress, when we examined association of Cdc45 in *mms1*Δ and *mms22*Δ strains by ChIP/qPCR we detected a twofold decrease in Cdc45 at early-firing origins of replication (unpublished data). We propose that Mms1 and Mms22, likely in complex with Rtt101, function to stabilize the replisome (Figure 8). Dissociation of the replisome from a subset of replication forks results in the replication defects we have observed in *mms1*Δ and *mms22*Δ.

It is not clear why the levels of Mrc1, Csm3, and Dpb3 at HU-stalled replication forks decrease by only twofold in *mms1*Δ and *mms22*Δ strains. It is possible that some forks are refractory to the absence of Mms1 and Mms22, such that Mrc1, Csm3, and Dpb3 completely dissociate from some forks but are unaffected at others. If this is the case, it is unlikely that these forks represent a specific subset, because the binding signals were uniformly decreased across the genome. Rather, it is more likely to be a stochastic effect, where an effect at a given fork in one cell does not predict or reflect an effect at the same fork in a different cell. An alternative possibility is that the affinity of Mrc1, Csm3, and Dpb3 for the replisome is reduced but not eliminated at all forks. In either case the result would likely be a reduced capacity for resumption of DNA synthesis once the replication stress is removed. This is evident in the mitotic delay and reduced viability in *mms1*Δ and *mms22*Δ following recovery from HU.

Is a twofold decrease in fork residence of these proteins likely to have a biological consequence? Short HU exposures have little effect on the viability of cells lacking Mms1 or Mms22, but it is clear that even modest depletion of replisome components can have severe consequences in terms of genome integrity. For example, moderate depletion of DNA Polδ causes genome instability without obvious effects on growth rate (Lemoine *et al.*, 2008). Our data indicate that absence of Mms1 or Mms22, and the depletion of Mrc1, Csm3, and Dpb3 at stalled forks that results, causes a defect in DNA replication in the presence of HU and during recovery from HU.

MATERIALS AND METHODS

Yeast strains and media

Yeast strains used in this study are derivatives of BY4741 (Brachmann *et al.*, 1998) or W303 and are listed in Table 1. Standard yeast media and growth conditions were used (Sherman, 1991).

Hydroxyurea sensitivity assays

To measure sensitivity to continual exposure to HU, cells were grown in 5 ml of YPD overnight at 30°C, serially diluted 10-fold, and spotted onto YPD plates containing 0, 50, 100, 150, and 200 mM HU. Plates were incubated at 30°C for 2–3 d.

To measure sensitivity to acute HU exposure, cells were grown overnight at 30°C in 30 ml of YPD. Cells were then diluted and grown to early-log phase and treated with hydroxyurea at a final concentration of 200 mM. Samples were collected at the indicated time points and plated onto YPD to determine the number of colony-forming units. The average of two independent experiments was plotted.

Flow cytometry and mitotic index

Examination of DNA content in the presence of replication fork stress and during recovery from fork stalling was performed on a Guava flow cytometer (Millipore, Billerica, MA). Data were analyzed using FlowJo Flow Cytometry Analysis Software, version 9.0 (Ashland, OR). Histograms represent the cell cycle distribution of the indicated samples. The *y*-axis of each graph has been scaled to represent the percentage of the maximum bin contained in that profile. Samples were also processed for parallel analysis of nuclear morphology (Roberts *et al.*, 2006). In brief, log-phase cells were blocked in 2 μg/ml α-factor for 3 h at 23°C. Cells were then washed and resuspended in media containing 100 μg/ml pronase (Sigma-Aldrich, St. Louis, MO) and 200 mM HU (Sigma-Aldrich) for 90 min at 23°C with sampling every 30 min. Cells were then washed to remove HU, resuspended in YPD, and incubated for an additional 3 h at 23°C with sampling every 30 min. The 1-ml samples were fixed in 70% ethanol and stored at 4°C. For morphology analysis, 50 μl of cells were harvested, resuspended in 10 μl of VECTASHIELD mounting media with 4,6-diamidino-2-phenylindole (DAPI) (Vector Laboratories, Burlingame, CA), and imaged on a Zeiss Axiovert inverted microscope.

BrdU IP-chip, ChIP-chip, and qPCR

BrdU IP-chip and ChIP-chip experiments were performed essentially as described (Katou *et al.*, 2003, 2006; Roberts *et al.*, 2008). Signal intensity peak area was used to assess differences in ChIP-chip profiles between mutants and their respective wild-type controls. For each experiment, the $\log_2$ signal intensity values for probes 5000 base pairs on either side of each origin were extracted at 50-nucleotide intervals and the values summed as a measure of peak area. Twelve early-firing origins were selected, including 10 origins that were randomly chosen from the BrdU data (ARS305,

Strain	Genotype	Source
ABY8	*MAT***a** *DPB3-6HIS-10FLAG-KanMX mms22Δ::NatMX leu2Δ0 his3Δ1 ura3Δ0 met15Δ0*	This study
BY4741	*MAT***a** *leu2Δ0 his3Δ0 ura3Δ0 met15Δ0*	Brachmann *et al*. (1998)
CSM3-3FL	*MAT***a** *CSM3-6HIS-3FLAG-loxP-KanMX-loxP leu2Δ0 his3Δ0 ura3Δ0 met15Δ0*	Katou *et al*. (2003)
E1670	*MAT***a** *ade2-1 trp1-1 can1-100 his3-11,15 leu2-3112, RAD5+ GAL psi+ ura3::URA3/GPD-TK(7x)*	Etienne Schwob[a]
JOY128	*MAT***a** *DPB3-6HIS-10FLAG-KanMX leu2Δ0 his3Δ1 ura3Δ0 met15Δ0*	This study
JVY39	*MAT***a** *MMS1-6HIS-10FLAG-KanMX leu2Δ0 his3Δ0 ura3Δ0 met15Δ0*	This study
JVY54	*MAT***a** *MMS1-6HIS-10FLAG-KanMX rtt101Δ::NatMX leu2Δ0 his3Δ0 ura3Δ0 met15Δ0*	This study
JVY56	*MAT***a** *MMS1-6HIS-10FLAG-KanMX mms22Δ::NatMX leu2Δ0 his3Δ0 ura3Δ0 met15Δ0*	This study
JVY65	*MAT***a** *mms1Δ::NatMX ade2-1 trp1-1 can1-100 his3-11, 15 leu2-3112, RAD5+ GAL psi+ ura3::URA3/GDP-TK(7x)*	This study
JVY72	*MAT***a** *mms1Δ::NatMX leu2Δ0 his3Δ1 ura3Δ0 met15Δ0*	This study
JVY73	*MAT***a** *mms22Δ::NatMX leu2Δ0 his3Δ1 ura3Δ0 met15Δ0*	This study
JVY76	*MAT***a** *MRC1-6HIS-3FLAG-loxP-KanMX-loxP mms1Δ::NatMX leu2Δ0 his3Δ1 ura3Δ0 met15Δ0*	This study
JVY77	*MAT***a** *MRC1-6HIS-3FLAG-loxP-KanMX-loxP mms22Δ::NatMX leu2Δ0 his3Δ1 ura3Δ0 met15Δ0*	This study
JVY80	*MAT***a** *CSM3-6HIS-3FLAG-loxP-KanMX-loxP mms1Δ::NatMX leu2Δ0 his3Δ0 ura3Δ0 met15Δ0*	This study
JVY101	*MAT***a** *CSM3-6HIS-3FLAG-loxP-KanMX-loxP mms22Δ::NatMX leu2Δ0 his3Δ0 ura3Δ0 met15Δ0*	This study
JVY134	*MAT***a** *DPB3-6HIS-10FLAG-KanMX mms1Δ::NatMX leu2Δ0 his3Δ1 ura3Δ0 met15Δ0*	This study
JVY157	*MAT***a** *DPB3-6HIS-10FLAG-KanMX ade2-1 trp1-1 can1-100 his3-11,15 leu2-3112, RAD5+ GAL psi+ ura3::URA3/GPD-TK(7x)*	This study
JVY158	*MAT***a** *mms1Δ::NatMX DPB3-6HIS-10FLAG-KanMX ade2-1 trp1-1 can1-100 his3-11,15 leu2-3112, RAD5+ GAL psi+ ura3::URA3/GDP-TK(7x)*	This study
MRC1-3FL	*MAT***a** *MRC1-6HIS-3FLAG-loxP-KanMX-loxP leu2Δ0 his3Δ1 ura3Δ0 met15Δ0*	Katou *et al*. (2003)

[a]Montpellier Institute of Molecular Genetics, Montpellier, France.

TABLE 1: Strains used in this study.

ARS306, ARS315, ARS416, ARS606, ARS719, ARS737, ARS920, ARS1015, ARS1211), and ARS607 and ARS1018, which were used for qPCR analysis. The distributions of the signal intensity sums were subjected to the Mann–Whitney test to determine whether the distributions were significantly different ($p < 0.05$) and are presented as box plots. For quantification of signal by qPCR, input and IP samples of DNA from at least two independent chromatin immunoprecipitations were collected using the same procedure as for ChIP-chip. Following purification of the DNA using a QIAquick PCR Purification Kit (Qiagen, Valencia, CA), samples were quantified using the DyNAmo HS SYBR Green qPCR Kit (Finnzymes, ThermoFisher Scientific, Waltham, MA) in an Applied Biosystems (Foster City, CA) 7500 Real-Time PCR System. Primers for amplification of ARS607 and ARS609 have been previously described (Lengronne *et al*., 2006). Primer sequences were designed for the amplification of DNA proximal to ARS1018 (forward, 5′-TAA CAG AAA ATC CAG ATT TGT ACA GAA AGA-3′; reverse, 5′-ATA TGT AAC CGC AAC AGT AGC CAA-3′) and the interorigin region between ARS1009 and ARS1010 (forward, 5′-TGA ATT AGA TGC TCT TCT GTA TAC TTT CTT-3′; reverse, 5′-GGT ACA TTC ACC TTG GTT TTC AAA TAC GT-3′). Averages of at least two independent experiments were plotted with the SD.

Genetic Interaction Data

Quantitative genetic interactions were identified by synthetic genetic array (SGA) analysis (Costanzo *et al*., 2010) and measured as described elsewhere (Baryshnikova *et al*., 2010; Costanzo *et al*., 2010). Protein complexes were assessed for biases in either positive or negative genetic interactions among its members by using a monochromatic purity (MP) score, described elsewhere (Baryshnikova *et al*., 2010). Complexes exhibiting only positive genetic interactions will have an MP score of +1, whereas an MP-score of −1 corresponds to complexes composed exclusively of negative interactions. Complexes whose interactions reflect the background ratio of positive to negative interactions have an MP score equal to 0. The ratio of positive to negative interactions (monochromacity) occurring between pairs of protein complexes was assessed in a similar manner. Protein complex pairs were also assessed for overall enrichment of genetic interactions using a hypergeometric p value.

Immunoblotting

Five optical density units of mid-log-phase cells were fixed with 10% trichloroacetic acid (Sigma-Aldrich), and extracts were prepared as described (Roberts *et al*., 2008). For treatment with hydroxyurea, cells were grown to early log phase at 23°C, arrested in G1 with 2 μg/ml α-factor for 3 h, and synchronously released into 100 μg/ml pronase and 200 mM HU (Sigma-Aldrich) for 90 min before fixation and extract preparation. Proteins were resolved on SDS–PAGE and subjected to immunoblot analysis with monoclonal ANTI-FLAG M2-Peroxidase antibody (Sigma-Aldrich) or anti–phosphoglycerate kinase monoclonal antibody (Molecular Probes, Invitrogen, Carlsbad, CA). Immunoblots were developed using SuperSignal ECL (Pierce Chemical, Rockford, IL).

ACKNOWLEDGMENTS

We thank Yuki Katou and Katsu Shirahige for analysis of BrdU IP-chip and ChIP-chip data and Attila Balint for strain construction. This work was supported by Grant 020254 from the Canadian Cancer Society to G.W.B., by Genome Canada through the Ontario Genomics Institute as per research agreement 2004-OGI-3-01, the Canadian Institutes of Health Research as per research agreement MOP-57830, and the Natural Sciences and Engineering Research Council of Canada as per research agreement RGPIN 204899-06 to C.B., and by a Canadian Graduate Scholarship from the Natural Sciences and Engineering Research Council of Canada to J.V.

REFERENCES

Alcasabas AA *et al.* (2001). Mrc1 transduces signals of DNA replication stress to activate Rad53. Nat Cell Biol 3, 958–965.

Alvino GM, Collingwood D, Murphy JM, Delrow J, Brewer BJ, Raghuraman MK (2007). Replication in hydroxyurea: it's a matter of time. Mol Cell Biol 27, 6396–6406.

Aparicio OM, Weinstein DM, Bell SP (1997). Components and dynamics of DNA replication complexes in *S. cerevisiae*: redistribution of MCM proteins and Cdc45p during S phase. Cell 91, 59–69.

Araki Y, Kawasaki Y, Sasanuma H, Tye BK, Sugino A (2003). Budding yeast mcm10/dna43 mutant requires a novel repair pathway for viability. Genes Cells 8, 465–480.

Baldwin EL, Berger AC, Corbett AH, Osheroff N (2005). Mms22p protects *Saccharomyces cerevisiae* from DNA damage induced by topoisomerase II. Nucleic Acids Res 33, 1021–1030.

Bando M, Katou Y, Komata M, Tanaka H, Itoh T, Sutani T, Shirahige K (2009). Csm3, Tof1, and Mrc1 form a heterotrimeric mediator complex that associates with DNA replication forks. J Biol Chem 284, 34355–34365.

Baryshnikova A *et al.* (2010). Quantitative analysis of fitness and genetic interactions in yeast on a genome scale. Nat Methods 7, 1017–1024.

Ben-Aroya S, Agmon N, Yuen K, Kwok T, McManus K, Kupiec M, Hieter P (2010). Proteasome nuclear activity affects chromosome stability by controlling the turnover of mms22, a protein important for DNA repair. PLoS Genet 6, e1000852.

Bennett CB, Lewis LK, Karthikeyan G, Lobachev KS, Jin YH, Sterling JF, Snipe JR, Resnick MA (2001). Genes required for ionizing radiation resistance in yeast. Nat Genet 29, 426–434.

Bjergbaek L, Cobb JA, Tsai-Pflugfelder M, Gasser SM (2005). Mechanistically distinct roles for Sgs1p in checkpoint activation and replication fork maintenance. EMBO J 24, 405–417.

Brachmann CB, Davies A, Cost GJ, Caputo E, Li J, Hieter P, Boeke JD (1998). Designer deletion strains derived from *Saccharomyces cerevisiae* S288C: a useful set of strains and plasmids for PCR-mediated gene disruption and other applications. Yeast 14, 115–132.

Calzada A, Hodgson B, Kanemaki M, Bueno A, Labib K (2005). Molecular anatomy and regulation of a stable replisome at a paused eukaryotic DNA replication fork. Genes Dev 19, 1905–1919.

Chang M, Bellaoui M, Boone C, Brown GW (2002). A genome-wide screen for methyl methanesulfonate-sensitive mutants reveals genes required for S phase progression in the presence of DNA damage. Proc Natl Acad Sci USA 99, 16934–16939.

Cobb JA, Bjergbaek L, Shimada K, Frei C, Gasser SM (2003). DNA polymerase stabilization at stalled replication forks requires Mec1 and the RecQ helicase Sgs1. EMBO J 22, 4325–4336.

Cobb JA, Schleker T, Rojas V, Bjergbaek L, Tercero JA, Gasser SM (2005). Replisome instability, fork collapse, and gross chromosomal rearrangements arise synergistically from Mec1 kinase and RecQ helicase mutations. Genes Dev 19, 3055–3069.

Collins SR *et al.* (2007). Functional dissection of protein complexes involved in yeast chromosome biology using a genetic interaction map. Nature 446, 806–810.

Costanzo M *et al.* (2010). The genetic landscape of a cell. Science 327, 425–431.

Crabbe L, Thomas A, Pantesco V, De Vos J, Pasero P, Lengronne A (2010). Analysis of replication profiles reveals key role of RFC-Ctf18 in yeast replication stress response. Nat Struct Mol Biol 17, 1391–1397.

Desany BA, Alcasabas AA, Bachant JB, Elledge SJ (1998). Recovery from DNA replicational stress is the essential function of the S-phase checkpoint pathway. Genes Dev 12, 2956–2970.

Dovey CL, Aslanian A, Sofueva S, Yates JR 3rd, Russell P (2009). Mms1-Mms22 complex protects genome integrity in *Schizosaccharomyces pombe*. DNA Repair (Amst) 8, 1390–1399.

Dovey CL, Russell P (2007). Mms22 preserves genomic integrity during DNA replication in *Schizosaccharomyces pombe*. Genetics 177, 47–61.

Duro E, Vaisica JA, Brown GW, Rouse J (2008). Budding yeast Mms22 and Mms1 regulate homologous recombination induced by replisome blockage. DNA Repair (Amst) 7, 811–818.

Feng W, Collingwood D, Boeck ME, Fox LA, Alvino GM, Fangman WL, Raghuraman MK, Brewer BJ (2006). Genomic mapping of single-stranded DNA in hydroxyurea-challenged yeasts identifies origins of replication. Nat Cell Biol 8, 148–155.

Fujii K, Kitabatake M, Sakata T, Miyata A, Ohno M (2009). A role for ubiquitin in the clearance of nonfunctional rRNAs. Genes Dev 23, 963–974.

Gambus A, Jones RC, Sanchez-Diaz A, Kanemaki M, van Deursen F, Edmondson RD, Labib K (2006). GINS maintains association of Cdc45 with MCM in replisome progression complexes at eukaryotic DNA replication forks. Nat Cell Biol 8, 358–366.

Gambus A, van Deursen F, Polychronopoulos D, Foltman M, Jones RC, Edmondson RD, Calzada A, Labib K (2009). A key role for Ctf4 in coupling the MCM2-7 helicase to DNA polymerase alpha within the eukaryotic replisome. EMBO J 28, 2992–3004.

Higa LA, Mihaylov IS, Banks DP, Zheng J, Zhang H (2003). Radiation-mediated proteolysis of CDT1 by CUL4-ROC1 and CSN complexes constitutes a new checkpoint. Nat Cell Biol 5, 1008–1015.

Hiraga S, Hagihara-Hayashi A, Ohya T, Sugino A (2005). DNA polymerases alpha, delta, and epsilon localize and function together at replication forks in *Saccharomyces cerevisiae*. Genes Cells 10, 297–309.

Ho Y *et al.* (2002). Systematic identification of protein complexes in *Saccharomyces cerevisiae* by mass spectrometry. Nature 415, 180–183.

Hryciw T, Tang M, Fontanie T, Xiao W (2002). MMS1 protects against replication-dependent DNA damage in *Saccharomyces cerevisiae*. Mol Genet Genomics 266, 848–857.

Jackson S, Xiong Y (2009). CRL4s: the CUL4-RING E3 ubiquitin ligases. Trends Biochem Sci 34, 562–570.

Kapetanaki MG, Guerrero-Santoro J, Bisi DC, Hsieh CL, Rapic-Otrin V, Levine AS (2006). The DDB1-CUL4ADDB2 ubiquitin ligase is deficient in xeroderma pigmentosum group E and targets histone H2A at UV-damaged DNA sites. Proc Natl Acad Sci USA 103, 2588–2593.

Katou Y, Kaneshiro K, Aburatani H, Shirahige K (2006). Genomic approach for the understanding of dynamic aspect of chromosome behavior. Methods Enzymol 409, 389–410.

Katou Y, Kanoh Y, Bando M, Noguchi H, Tanaka H, Ashikari T, Sugimoto K, Shirahige K (2003). S-phase checkpoint proteins Tof1 and Mrc1 form a stable replication-pausing complex. Nature 424, 1078–1083.

Koh JL, Ding H, Costanzo M, Baryshnikova A, Toufighi K, Bader GD, Myers CL, Andrews BJ, Boone C (2010). DRYGIN: a database of quantitative genetic interaction networks in yeast. Nucleic Acids Res 38, D502–507.

Krakoff IH, Brown NC, Reichard P (1968). Inhibition of ribonucleoside diphosphate reductase by hydroxyurea. Cancer Res 28, 1559–1565.

Lemoine FJ, Degtyareva NP, Kokoska RJ, Petes TD (2008). Reduced levels of DNA polymerase delta induce chromosome fragile site instability in yeast. Mol Cell Biol 28, 5359–5368.

Lengronne A, McIntyre J, Katou Y, Kanoh Y, Hopfner KP, Shirahige K, Uhlmann F (2006). Establishment of sister chromatid cohesion at the *S. cerevisiae* replication fork. Mol Cell 23, 787–799.

Leung-Pineda V, Huh J, Piwnica-Worms H (2009). DDB1 targets Chk1 to the Cul4 E3 ligase complex in normal cycling cells and in cells experiencing replication stress. Cancer Res 69, 2630–2637.

Lopes M, Cotta-Ramusino C, Pellicioli A, Liberi G, Plevani P, Muzi-Falconi M, Newlon CS, Foiani M (2001). The DNA replication checkpoint response stabilizes stalled replication forks. Nature 412, 557–561.

Lou H, Komata M, Katou Y, Guan Z, Reis CC, Budd M, Shirahige K, Campbell JL (2008). Mrc1 and DNA polymerase epsilon function together in linking DNA replication and the S phase checkpoint. Mol Cell 32, 106–117.

Lucca C, Vanoli F, Cotta-Ramusino C, Pellicioli A, Liberi G, Haber J, Foiani M (2004). Checkpoint-mediated control of replisome-fork association and signalling in response to replication pausing. Oncogene 23, 1206–1213.

Luke B, Versini G, Jaquenoud M, Zaidi IW, Kurz T, Pintard L, Pasero P, Peter M (2006). The cullin Rtt101p promotes replication fork progression through damaged DNA and natural pause sites. Curr Biol 16, 786–792.

Michel JJ, McCarville JF, Xiong Y (2003). A role for *Saccharomyces cerevisiae* Cul8 ubiquitin ligase in proper anaphase progression. J Biol Chem 278, 22828–22837.

Mimura S, Komata M, Kishi T, Shirahige K, Kamura T (2009). SCF(Dia2) regulates DNA replication forks during S-phase in budding yeast. EMBO J 28, 3693–3705.
Mimura S, Yamaguchi T, Ishii S, Noro E, Katsura T, Obuse C, Kamura T. (2010). Cul8/Rtt101 forms a variety of protein complexes that regulate DNA damage response and transcriptional silencing. J Biol Chem 285, 9858–9867.
Naylor ML, Li JM, Osborn AJ, Elledge SJ (2009). Mrc1 phosphorylation in response to DNA replication stress is required for Mec1 accumulation at the stalled fork. Proc Natl Acad Sci USA 106, 12765–12770.
Nedelcheva MN, Roguev A, Dolapchiev LB, Shevchenko A, Taskov HB, Stewart AF, Stoynov SS (2005). Uncoupling of unwinding from DNA synthesis implies regulation of MCM helicase by Tof1/Mrc1/Csm3 checkpoint complex. J Mol Biol 347, 509–521.
Nick McElhinny SA, Gordenin DA, Stith CM, Burgers PM, Kunkel TA (2008). Division of labor at the eukaryotic replication fork. Mol Cell 30, 137–144.
Noguchi E, Noguchi C, McDonald WH, Yates JR 3rd, Russell P. (2004). Swi1 and Swi3 are components of a replication fork protection complex in fission yeast. Mol Cell Biol 24, 8342–8355.
Osborn AJ, Elledge SJ (2003). Mrc1 is a replication fork component whose phosphorylation in response to DNA replication stress activates Rad53. Genes Dev 17, 1755–1767.
Pan X, Ye P, Yuan DS, Wang X, Bader JS, Boeke JD (2006). A DNA integrity network in the yeast *Saccharomyces cerevisiae*. Cell 124, 1069–1081.
Plevani P, Badaracco G, Augl C, Chang LM (1984). DNA polymerase I and DNA primase complex in yeast. J Biol Chem 259, 7532–7539.
Pursell ZF, Isoz I, Lundstrom EB, Johansson E, Kunkel TA (2007). Yeast DNA polymerase epsilon participates in leading-strand DNA replication. Science 317, 127–130.
Ricke RM, Bielinsky AK (2004). Mcm10 regulates the stability and chromatin association of DNA polymerase-alpha. Mol Cell 16, 173–185.
Roberts TM *et al*. (2006). Slx4 regulates DNA damage checkpoint-dependent phosphorylation of the BRCT domain protein Rtt107/Esc4. Mol Biol Cell 17, 539–548.
Roberts TM, Waris Zaidi I, Vaisica JA, Peter M, Brown GW (2008). Regulation of Rtt107 recruitment to stalled DNA replication forks by the cullin Rtt101 and the Rtt109 acetyltransferase. Mol Biol Cell 19, 171–180.
Sherman F (1991). Getting started with yeast. Methods Enzymol 194, 3–21.
Shimmoto M, Matsumoto S, Odagiri Y, Noguchi E, Russell P, Masai H (2009). Interactions between Swi1-Swi3, Mrc1 and S phase kinase, Hsk1 may regulate cellular responses to stalled replication forks in fission yeast. Genes Cells 14, 669–682.
Singh H, Dumas LB (1984). A DNA primase that copurifies with the major DNA polymerase from the yeast *Saccharomyces cerevisiae*. J Biol Chem 259, 7936–7940.
Slater ML (1973). Effect of reversible inhibition of deoxyribonucleic acid synthesis on the yeast cell cycle. J Bacteriol 113, 263–270.
Sogo JM, Lopes M, Foiani M (2002). Fork reversal and ssDNA accumulation at stalled replication forks owing to checkpoint defects. Science 297, 599–602.
Sugasawa K *et al*. (2005). UV-induced ubiquitylation of XPC protein mediated by UV-DDB-ubiquitin ligase complex. Cell 121, 387–400.
Suter B *et al*. (2007). Examining protein protein interactions using endogenously tagged yeast arrays: the cross-and-capture system. Genome Res 17, 1774–1782.
Szyjka SJ, Viggiani CJ, Aparicio OM (2005). Mrc1 is required for normal progression of replication forks throughout chromatin in *S. cerevisiae*. Mol Cell 19, 691–697.
Takayama Y, Kamimura Y, Okawa M, Muramatsu S, Sugino A, Araki H (2003). GINS, a novel multiprotein complex required for chromosomal DNA replication in budding yeast. Genes Dev 17, 1153–1165.
Tanaka H, Katou Y, Yagura M, Saitoh K, Itoh T, Araki H, Bando M, Shirahige K (2009). Ctf4 coordinates the progression of helicase and DNA polymerase alpha. Genes Cells 14, 807–820.
Tercero JA, Labib K, Diffley JF (2000). DNA synthesis at individual replication forks requires the essential initiation factor Cdc45p. EMBO J 19, 2082–2093.
Tercero JA, Longhese MP, Diffley JF (2003). A central role for DNA replication forks in checkpoint activation and response. Mol Cell 11, 1323–1336.
Tittel-Elmer M, Alabert C, Pasero P, Cobb JA (2009). The MRX complex stabilizes the replisome independently of the S phase checkpoint during replication stress. EMBO J 28, 1142–1156.
Torres-Rosell J *et al*. (2007). Anaphase onset before complete DNA replication with intact checkpoint responses. Science 315, 1411–1415.
Tourriere H, Versini G, Cordon-Preciado V, Alabert C, Pasero P (2005). Mrc1 and Tof1 promote replication fork progression and recovery independently of Rad53. Mol Cell 19, 699–706.
Wang H, Zhai L, Xu J, Joo HY, Jackson S, Erdjument-Bromage H, Tempst P, Xiong Y, Zhang Y (2006). Histone H3 and H4 ubiquitylation by the CUL4-DDB-ROC1 ubiquitin ligase facilitates cellular response to DNA damage. Mol Cell 22, 383–394.
Weinert TA, Kiser GL, Hartwell LH (1994). Mitotic checkpoint genes in budding yeast and the dependence of mitosis on DNA replication and repair. Genes Dev 8, 652–665.
Yokoyama M, Inoue H, Ishii C, Murakami Y (2007). The novel gene mus7(+) is involved in the repair of replication-associated DNA damage in fission yeast. DNA Repair (Amst) 6, 770–780.
Zaidi IW *et al*. (2008). Rtt101 and Mms1 in budding yeast form a CUL4(DDB1)-like ubiquitin ligase that promotes replication through damaged DNA. EMBO Rep 9, 1034–1040.
Zou L, Stillman B (2000). Assembly of a complex containing Cdc45p, replication protein A, and Mcm2p at replication origins controlled by S-phase cyclin-dependent kinases and Cdc7p-Dbf4p kinase. Mol Cell Biol 20, 3086–3096.